

# Fractal asymptotics

C. P. Dettmann\*

November 16, 2018

## Abstract

Recent advances in the periodic orbit theory of stochastically perturbed systems have permitted a calculation of the escape rate of a noisy chaotic map to order 64 in the noise strength. Comparison with the usual asymptotic expansions obtained from integrals and with a previous calculation of the electrostatic potential of exactly selfsimilar fractal charge distributions, suggests a remarkably accurate form for the late terms in the expansion, with parameters determined independently from the fractal repeller and the critical point of the map. Two methods give a precise meaning to the asymptotic expansion, Borel summation and Shafer approximants. These can then be compared to the escape rate as computed by alternative methods.

Keywords: Asymptotic expansions, Borel summation, Padé approximation, cycle expansions, escape rates, fractals, maps, repellers, stochastic perturbations.

PACS: 02.30.Mv 05.40.Ca 05.45.Df

## 1 Introduction

Fractal sets and measures appear naturally as invariant sets (respectively measures) of many nonlinear dynamical systems. Periodic orbit theory [1] provides an effective approach to computing useful properties such as averages, Lyapunov exponents and dimensions, particularly when the fractal corresponds to a nonattracting set (“transient chaos”) so that direct simulation methods are harder to implement. In the case of Axiom A dynamics, the convergence of periodic orbit (or “cycle”) expansions can be spectacular, see Tab. 1 below.

Recent work has extended the theory to include chaotic systems perturbed by external noise, motivated by realism (all physical systems are coupled to unknown degrees of freedom) and smoothness (delta functions are replaced by smooth distributions). While

---

\*Department of Mathematics, University of Bristol, University Walk Bristol BS8 1TW, UK

several approaches have been attempted, including Feynman diagrams [2] (by analogy with quantum perturbation theory) and smooth conjugations [3] (by analogy with classical perturbation theory), the most computationally effective method [4] has been to represent the stochastic evolution (Fokker-Planck) operator by a matrix in a basis of polynomials about each periodic orbit, truncated to finite size using the fact that the elements decay exponentially, that is, the eigenfunctions are very smooth.

The previous work [4] computed the escape rate of a stochastically perturbed map to order 8 in the noise strength. In this paper the same matrix method, extended to high (60 digit) precision arithmetic, is used to compute the escape rate to order 64 in the noise strength. With this number of coefficients, it is meaningful to consider the asymptotic form of the late terms, the subject of this paper.

We will discover that to unlock the secrets of the noise expansion will require insights not only from the classical theory of asymptotic expansions, but also from more recent analytic calculations involving fractals. The relatively small number of numerical coefficients is compensated by their high precision, allowing a reliable fit to a functional form involving several parameters. Comparing two interpretations of the series, Borel summation and Shafer (generalised Padé) approximation to the “exact” function, we will find that exponentially small corrections will need to be considered by a future theory.

At this point we note a few other relevant works. Contour integration methods [5] have obtained the asymptotic form of noise coefficients for fixed periodic orbit length, however this does not directly determine the noise expansion of the escape rate since the latter requires successively longer orbits for higher noise corrections. Direct integration [6] has shown numerically that the cumulant expansion on which the cycle expansions are based is valid for strong as well as weak noise. Stochastically perturbed dynamical systems constitute a vast field, applying many methods other than periodic orbit theory.

Section 2 outlines the previous theory and methods needed to understand the results and their interpretation. For space reasons, readers interested in the full details are referred to the original works. Section 3 gives the coefficients, the logic used to fit them to a particular functional form, and the Borel summation or Shafer approximation needed to assign a precise meaning to the asymptotic expansion. Final discussion is given in section 4.

## 2 Preliminaries

### 2.1 Asymptotic series

This subsection gives the background for asymptotic series. A very readable review of this subject and its applications is given by Boyd [7]. Singular perturbations of integrals or differential equations, such as perturbative approaches to physical problems, frequently have power series expansions of the form

$$\sum_m (m + \alpha)! \left(\frac{x}{x_0}\right)^m M_m \tag{1}$$

where  $\alpha$  is often an integer or half integer, and  $x_0$  (or rather its inverse) is called the *singulant*, and is related to the nearest critical point of an integrand.  $M_m$  is called the *modifying factor* and tends to a constant as  $m \rightarrow \infty$ ; it contains all the slower varying functional behaviour.

Such series diverge for all  $x \neq 0$ , and a number of methods have been employed to make sense of them. The simplest (albeit discontinuous) is to truncate the sum at its smallest term. An alternative, which Boyd states as usually the most computationally efficient, is to replace the series by its Padé approximants, more specifically the Shafer extension [8] in which the function is written as the solution of a quadratic equation with polynomial coefficients; the coefficients of the polynomials are found by a set of (typically ill-conditioned) linear equations.

While Padé methods give results on average as good as any other method to this order, an alternative, Borel summation, offers the possibility of systematic exponentially accurate (“hyperasymptotic”) corrections. These methods (for example Berry and Howls [9]) start from the Borel summation method as formulated by Dingle [10], which we follow. The latter retains the decreasing terms, then performs Borel summation on the divergent “tail”. Borel summation is an approach in which the factorial is replaced by its integral representation [11], and the sum and integral are interchanged. In the present context, where the terms are all the same complex phase, this leads to a pole in the path of integration (corresponding to a “Stokes line”); the constraint that the result must be real then indicates that the principal value of the integral should be taken. Dingle also shows how to write the Borel summed expression in terms of a few standard functions (related to incomplete gamma functions [11]) which he calls *terminants*; we use his method based on the forward difference expansion. More details can be found in Dingle’s book [10].

For the bulk of this paper, we will need only Eq. (1), in order to fit the parameters, and generalise it slightly. Once the form for the coefficients has been established, the Shafer and Dingle methods will be applied, and compared with the “exact” numerical result; the Shafer method gives marginally more accurate results. Since the coefficients are fitted, not known exactly, and our calculation does not attempt to identify exponentially small corrections (although this should be possible in the future), we cannot apply the more detailed hyperasymptotic methods of Berry and Howls [9] and others (refer to Ref. [7] for extensive references). Nevertheless, we succeed in computing a function accurate to remarkably high values of the noise strength (perturbation parameter).

## 2.2 Exactly self-similar fractals

This subsection gives the background for analytic expansions pertaining to exactly self-similar fractals, giving additional clues to the value of the parameter  $\alpha$  in Eq. (1) and generalisations of this equation that we might expect for the noise expansion in later sections. The first paper to introduce asymptotic methods applied to a fractal problem [12] discussed Julia sets, but is more technically involved than the exactly self-similar fractals in Refs. [13, 14]. The discussion in this section is based on Ref. [13].

The middle-third Cantor set consists of two copies of itself scaled down by a factor of three, thus it has dimension  $d = \ln 2 / \ln 3$  according to many definitions. The uniform measure on the set located between  $x = \pm 1/2$  satisfies the relation

$$\int f(x) d\mu(x) = \frac{1}{2} \int \left[ f\left(\frac{x-1}{3}\right) + f\left(\frac{x+1}{3}\right) \right] d\mu(x) \quad (2)$$

for arbitrary smooth function  $f(x)$ , which together with the definitions of the electrostatic potential

$$V(x) = \int \frac{d\mu(x')}{|x-x'|} \quad (3)$$

and the moments

$$C_n = \int x^n d\mu(x) \quad (4)$$

lead after several steps [13] to the following expression for the potential near the edge of the fractal,

$$V(1/2 + \xi) = \xi^{d-1} \sum_{p=0}^{\infty} a_p \cos\left(\frac{2\pi p}{\ln 3} \ln \xi + \phi_p\right) + \sum_{p=0}^{\infty} b_p \xi^p \quad (5)$$

where  $a_p$ ,  $b_p$  and  $\phi_p$  are known series given in terms of the  $C_n$ , which are in turn given as explicit rational numbers with a well understood asymptotic form. The  $a_p$  have a large exponential decay rate for example  $a_0 = 1.7685$ ,  $a_1 = 7.04977 \times 10^{-8}$ ,  $a_2 = 6.7575 \times 10^{-17}$ . The oscillatory terms come from the  $p \neq 0$  solutions

$$d = \frac{\ln 2}{\ln 3} + \frac{2\pi ip}{\ln 3} \quad (6)$$

of the equation  $3^d = 2$  defining the dimension. Such “complex dimensions” of fractals appear in a number of physical applications [15].

Even though the context is different from that of the noise corrections considered below in Sec. 3.3, in particular the expansion for the potential has a finite radius of convergence while that of the noise is divergent, we may conjecture that there are a number of general principles applying to fractal expansions. In particular, the leading order of the expansion is not a single term but a sum of terms containing a variable (here  $\xi$ ) raised to powers  $\alpha + ip\beta$  for all integers  $p$ , where  $\alpha$  and  $\beta$  are determined by properties of the fractal:

1. The parameter  $\alpha$  (here  $d - 1$ ) is related to the dimension of the fractal.
2. The parameter  $\beta$  (here  $2\pi/\ln 3$ ) is determined by the spatial scaling factor 3 of the fractal.
3. Due to the rapid decay of the oscillatory coefficients, accurate results may be obtained by considering only one or two of these terms, ie  $|p| \leq 1$ .

Note that in the absence of the imaginary  $\beta$  terms (perhaps a “nonfractal limit”), the  $\alpha$  in this section corresponds to the  $\alpha$  in Eq. (1) since the latter effectively has  $\alpha$  in the exponent:  $(m + \alpha)! \sim m! m^\alpha$  as  $m \rightarrow \infty$ .

### 2.3 Periodic orbit theory of stochastically perturbed maps

This subsection gives a background to the numerical coefficients discussed in the main part of the paper. The periodic orbit theory [1] allows the computation of long time properties such as averages, Lyapunov exponents, and correlation functions from periodic orbits. The required properties are related to the leading eigenvalue(s) of an evolution operator (defined below), which, in the most rapidly convergent formulation, are computed using determinants. The determinant is expressed as an expansion in traces, and the traces are expressed in terms of periodic orbits.

Consider the discrete time dynamics described by

$$x_{n+1} = f(x_n) + \sigma \xi_n \quad (7)$$

where  $\sigma$  is the noise strength and  $\xi_n$  are instances of an uncorrelated random variable. In the present case  $x$  is a real number, but higher dimensional generalisations are straightforward, at least in the deterministic case  $\sigma = 0$ . Continuous time dynamics can also be considered; the stochastic version has been discussed in Ref. [16]. The probability density  $\rho(x)$  evolves according to

$$\rho_{n+1}(y) = (\mathcal{L} \circ \rho_n)(y) = \int \rho_n(x) \delta_\sigma(y - f(x)) dx \quad (8)$$

where  $\mathcal{L}$  as defined above is the (discrete time Fokker-Planck) evolution operator. The noise distribution  $\delta_\sigma(z)$  is an arbitrary function of standard deviation  $\sigma$ ; it reduces to a Dirac delta in the deterministic case  $\sigma = 0$ . We compute the trace

$$\text{tr} \mathcal{L}^n = \int dx_0 dx_1 \dots dx_{n-1} \delta_\sigma(x_1 - f(x_0)) \delta_\sigma(x_2 - f(x_1)) \dots \delta_\sigma(x_0 - f(x_{n-1})) \quad (9)$$

which is an  $n$ -dimensional integral. In the deterministic case, it reduces to a sum over periodic points  $x$  satisfying  $f^n(x) = x$  of the relevant Jacobian. The weak noise theory is effectively a stationary phase approximation in which the leading order behaviour is given by the deterministic limit, with corrections determined by higher derivatives of the map  $f(x)$  evaluated at the periodic points. Exponentially small corrections are obtained by considering local extrema, which are given by the ‘‘generalised periodic orbits’’ of [5], that is, periodic orbits of the extended system  $(x, p) \rightarrow (f(x) + p/f'(x), p/f'(x))$ ; these will be discussed later.

The characteristic determinant is

$$0 = \det(1 - z\mathcal{L}) = \exp \text{tr} \ln(1 - z\mathcal{L}) = 1 - z \text{tr} \mathcal{L} - \frac{z^2}{2} (\text{tr} \mathcal{L}^2 - (\text{tr} \mathcal{L})^2) + \dots \quad (10)$$

where we define the determinant in terms of its expansion in powers of the inverse eigenvalue  $z$ ; this is consistent with our desire for the largest eigenvalue (smallest  $z$ ). The eigenvalue itself can be obtained by truncating the above equation at some  $z^n$ , which requires computing periodic orbits up to length  $n$ , and solving numerically for the first

zero. The leading eigenvalue  $\nu = z^{-1}$  has a direct interpretation: the quantity  $\gamma = -\ln \nu$  is the escape rate, that is, a uniform distribution of initial conditions leads to a number proportional to  $\exp(-\gamma n)$  remaining at long times  $n \gg 1$ . Other useful quantities can be obtained by small modifications of the method, for example weighting the evolution operator using the function for which an average is desired.

We note that because the eigenvalue is not directly expressed as an integral, rather an expansion of integrals or the infinite dimensional limit of an integral, the Dingle theory discussed in Sec. 2.1 does not strictly apply. In principle (although not in practice) an infinite number of critical points are required to determine the eigenvalue.

There have been two analytical approaches to evaluating the integral for the trace in the stochastic case, in particular Feynman diagrams [2] and smooth conjugations [3]. These give the trace explicitly in terms of the derivatives of  $f(x)$  at the periodic points, but have been applied only up to order  $\sigma^4$ . A more numerical approach was used in Ref. [4] to obtain coefficients up to  $\sigma^8$ , and it is the latter approach which is used in this paper.

The evolution operator is expressed in an explicit polynomial basis (in contrast to the usual situation in periodic orbit theory, where all calculations are kept independent of the basis), defined in the vicinity of each periodic point. Truncating the representation to a finite matrix is justified since the eigenfunction is very smooth, leading to exponential decay of the matrix elements. All quantities are expanded in powers of the small parameter  $\sigma$ , and the full trace is obtained as a sum over periodic points, to each order in  $\sigma$ . Finally the leading eigenvalue is obtained as a formal power series

$$\nu(\sigma) = \sum_{m=0}^{\infty} \nu_{2m} \sigma^{2m} \quad (11)$$

where odd powers vanish by the symmetry of the Gaussian noise distribution used. Further details of the calculation are given in Ref. [4].

## 3 Results

### 3.1 Numerical details

In the previous paper [4] the results were limited to  $\sigma^8$  since high precision is required (the cumulant expansion (10) involves many cancellations), and commercial high precision mathematical packages required too much memory and time. The results of this paper were achieved by code written in C, involving 60 digits precision, a maximum matrix size of 200 (the largest matrices are required for the shortest orbits) and periodic points up to  $n = 10$ . The matrix size for each orbit length and the maximum length were determined adaptively; the precision was estimated conservatively using the results of shorter calculations. Here, as in previous calculations [2, 3, 4], the noise is Gaussian, and

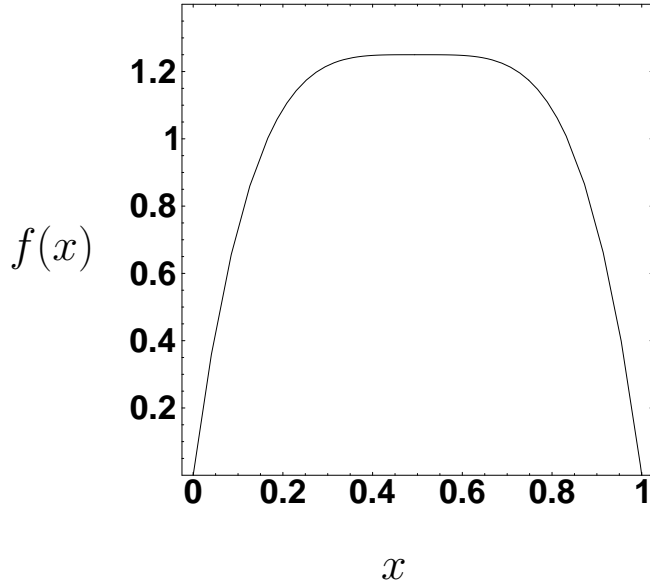


Figure 1: The map (12) appearing in (7).

$n$	$\nu_0$	$\nu_2$	$\nu_4$	$\nu_{64}$
1	0.307735902965	0.421227543767	2.15906608736	$1.397115735 \times 10^{53}$
2	0.371401067274	1.421640613096	32.97365355137	$5.001186917 \times 10^{75}$
3	0.371109569907	1.435552381965	36.32563272348	$2.001067045 \times 10^{80}$
4	0.371110995255	1.435811262322	36.35837768356	$2.651047356 \times 10^{80}$
5	0.371110995235	1.435811248197	36.35837123374	$2.660918038 \times 10^{80}$
6	0.371110995235	1.435811248197	36.35837123384	$2.660918375 \times 10^{80}$

Table 1: The noise coefficients of the eigenvalue, as defined in Eq. (11), calculated using periodic orbits up to length  $n$ .

the map appearing in (7) is

$$f(x) = 20 \left[ \frac{1}{16} - \left( \frac{1}{2} - x \right)^4 \right] \quad (12)$$

This map is Axiom A with complete binary symbolic dynamics, so the rate of convergence of the cycle expansion with orbit length is super-exponential, both for  $\nu_0$  (the deterministic case) and the noise corrections. Examples of this convergence (noted in the previous studies) are given in Tab. 1. The results for orbit length  $n = 10$ , expressed as the logarithms of the (always positive)  $\nu_{2m}$  are given in Tab. 2.

$2m$	$\ln \nu_{2m}$	$2m$	$\ln \nu_{2m}$	$2m$	$\ln \nu_{2m}$
0	-0.99125408258905	22	49.59463191979195	44	117.84381872333873
2	0.36173001922727	24	55.44039700516978	46	124.39362242853359
4	3.59342447275687	26	61.37352232130161	48	130.98895554172700
6	7.63842801043723	28	67.38731548909859	50	137.62787534158868
8	12.15107844830820	30	73.47605210071374	52	144.30858981612283
10	16.97610609587220	32	79.63476897706259	54	151.02944299196041
12	22.03308958456985	34	85.85911504876676	56	157.78889107050155
14	27.27470590323921	36	92.14524039569617	58	164.58550964455421
16	32.67034394383728	38	98.48971155485100	60	171.41796376702617
18	38.19872657460701	40	104.88944552922095	62	178.28500846576056
20	43.84418495656653	42	111.34165748821478	64	185.18547875658766

Table 2: The natural logarithm of the noise coefficients of the eigenvalue, as defined in Eq. (11). All  $\nu_{2m}$  are positive.

### 3.2 Fitting $\nu_{2m}$ to the form (1)

We immediately note that, while the coefficients  $\nu_{2m}$  converge very rapidly with orbit length  $n$ , they diverge with order  $m$ . This is not surprising since the noise expansion of the eigenvalue is effectively a stationary phase expansion of an integral, albeit with an infinite number of critical points. See Secs. 2.1, 2.3. A little curve fitting leads to the very approximate form

$$\nu(\sigma) = \sum \nu_{2m} \sigma^{2m} \approx \sum m! 32^m \sigma^{2m} \quad (13)$$

that is,  $\alpha = 0$  and  $\sigma_0 = 32^{-1/2}$  by comparison with (1). We would like to know the form of the coefficients more precisely than this, and in particular predict them from other information about the dynamics.

From the general theory of asymptotic expansions (Sec. 2.1) the singulant  $\sigma_0$  is somehow related to the distance between the critical point we are expanding around (periodic orbits on the fractal repeller) and the nearest critical point. In the present situation, if we consider the critical point of the original map (12) at  $x_c = 1/2$ , and ask for the probability for returning to the repeller, of which the most accessible point is  $x_r = 1$ , to first approximation this is

$$\exp \left[ -(x_r - f(x_c))^2 / 2\sigma^2 \right] = \exp \left[ -1/32\sigma^2 \right] \quad (14)$$

which indeed gives the 32. The reason that the singulant  $\sigma_0$  should be related to the coefficient of an exponential is that this exponentially small quantity (for small  $\sigma$ ), is, up to slower varying factors, the magnitude of the smallest term in the expansion, and hence the order at which exponentially small hyperasymptotic terms might contribute.

The above expression assumes that the transition from the critical point  $x = 1/2$  to the repeller  $x = 1$  takes place in a single step. Actually, for sufficiently small noise,



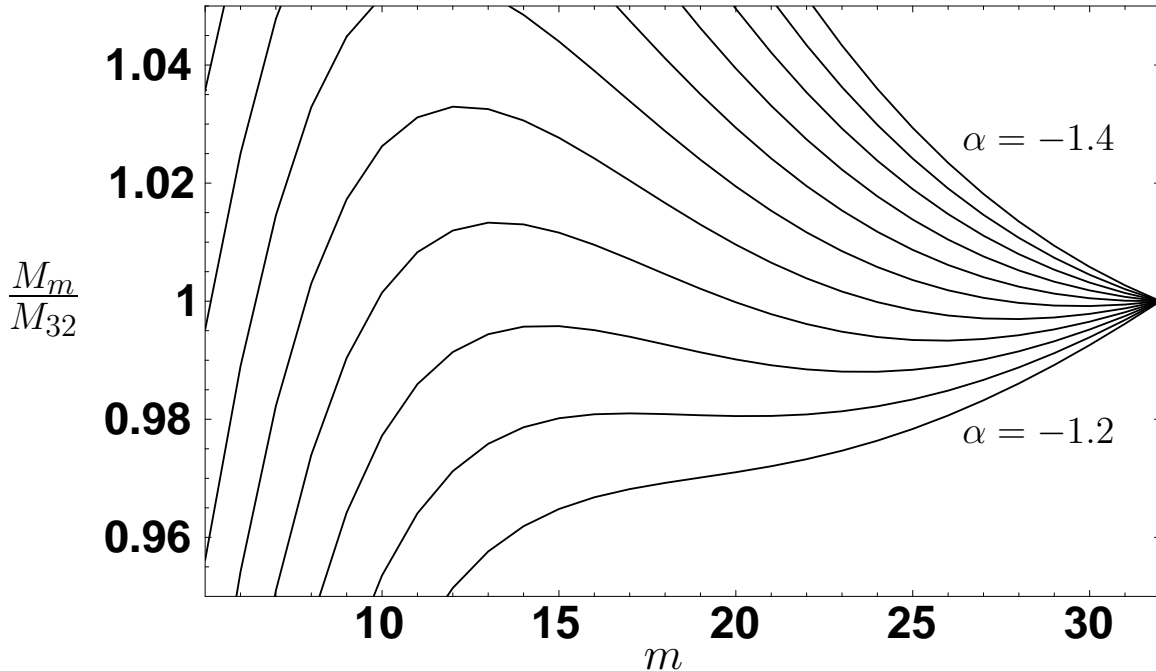


Figure 2: Attempt to fit the  $\nu_{2m}$  to a single asymptotic series of the canonical form. See Eq. (15). For none of the  $\alpha$  do the coefficients asymptote to a convincing horizontal line.

longer trajectories may be more likely. The probability is of the form  $\exp[-\sum(x_{n+1} - f(x_n))^2/2\sigma^2]$  which can be maximised over all trajectories starting at the critical point  $x = 1/2$  and reaching the repeller in the infinite time limit. The result is  $\sigma_0 = 32.31850341240166^{-1/2}$  for the trajectory  $\{0.5, 1.00244613635157, -0.00024587488150, -2.460023246 \times 10^{-5}, -2.46015082 \times 10^{-6}, -2.4601636 \times 10^{-7}, -2.460165 \times 10^{-8}, \dots, 0\}$ . The approach to zero is geometric with ratio  $f'(0)^{-1} = 1/10$ .

Another interpretation of this orbit is as the infinite length limit of a sequence of generalised periodic orbits (Sec. 2.3), responsible for exponentially small corrections to the traces; see later discussion in Sec. 3.4. For the rest of this paper, we assume that the 32 in Eq. (13) is replaced by the adjusted value  $\sigma_0^{-2} = 32.3185\dots$

The only remaining parameter to be fitted then seems to be the  $\alpha$  appearing in (1). With this in mind, we plot the quantity

$$M_m = \frac{\nu_{2m}\sigma_0^{2m}}{(m + \alpha)!} \quad (15)$$

normalised to the highest order  $M_{32}$  for various  $\alpha$  in Fig. 2.

As Fig. 2 shows, the  $M_m$  do not approach a constant for any value of  $\alpha$ . Even for the  $\alpha \approx -1.3$  at which the curve is roughly horizontal for the largest  $m$ , the curvature (as measured by the second derivative) is still large. There appears to be some oscillatory behaviour evident.

$q$	$-\infty$	0	1	2	$\infty$
$D_q$	0.5695	0.4007	0.3872	0.3757	0.2957

Table 3: Renyi dimensions of the fractal repeller, computed using periodic orbit theory.

### 3.3 Oscillations from complex exponents

At this point we recall the discussion of Sec. 2.2, in particular the three observations relating to fractal expansions at the end of that section. If we can identify  $\alpha$  in some way with the dimension of the fractal (at least in the Cantor set example), the oscillations noted at the end of the previous section appear naturally from a sum (over  $p$ ) of terms of the form  $(m + \alpha + ip\beta)!$  for integer  $p$ . Since the real part of  $\alpha + ip\beta$  is a constant  $\alpha$ , all of these terms are of the same order in the large  $m$  limit.

We return later to first observation in Sec. 2.2, that is, the question of whether  $\alpha$  is related to one of the fractal repeller's many dimensions, and leave it as a free parameter for the present. The second observation suggests that we look at the spatial scaling factor of the fractal repeller. The orbit discussed in the previous section reaches the fractal repeller at  $x = 0$ ; at this point the repeller is selfsimilar with a scaling factor of  $f'(0) = 10$ ; the same scaling factor that appears in the critical orbit of the previous section. The second observation of Sec. 2.2 then suggests  $\beta = 2\pi/\ln 10$ , which matches the oscillations well (see below). The third observation suggests that only small  $p$  may lead to sizable contributions, hence we will ignore  $|p| \geq 2$  and only include the real  $\alpha$  and a single pair of complex conjugates  $\alpha \pm i\beta$ .

We thus fit the data, as represented by the  $M_m$  of Eq. (15) to the function

$$c_0 + c_1 \frac{(m + \alpha + 2\pi i / \ln 10)!}{(m + \alpha)!} + c_1^* \frac{(m + \alpha - 2\pi i / \ln 10)!}{(m + \alpha)!} \quad (16)$$

where the  $*$  indicates complex conjugation,  $c_0$  is a real fit parameter and  $c_1$  is a complex fit parameter. Note that dividing through by  $(m + \alpha)!$  in Eq. (15) permits a linear (hence more reliable) fit for  $c_0$  and  $c_1$ . This fit is made for a range of values of  $\alpha$ , and for  $m_{\min} < m < 32$  with various  $m_{\min}$ . The error (in the least squares sense)  $\chi^2$  is given in Fig. 3, which shows an improvement limited by the precision of the results (14 decimal places in Tab. 2). From the optimal fit, we have  $\alpha = -1.290$ , corresponding to  $c_0 = 0.045514$  and  $c_1 = 0.000958 + 0.000185i$ . This fit is shown in Fig. 4.

We now return to the question of whether  $\alpha$  is related to a dimension of the fractal repeller. The Renyi generalised dimensions  $D_q$  of the repeller are straightforward to compute using the usual periodic orbit theory of deterministic systems [1]. The results are given in Tab. 3, but do not seem to exactly match our fitted value  $\alpha = -1.290$ . The closest is  $D_\infty$  (or rather  $-1 - D_\infty$ ), however this corresponds to the most stable periodic orbit which is the fixed point at  $x \approx 0.871$ , not the (most unstable) point  $x = 0$  used in the above calculation of the complex exponents.

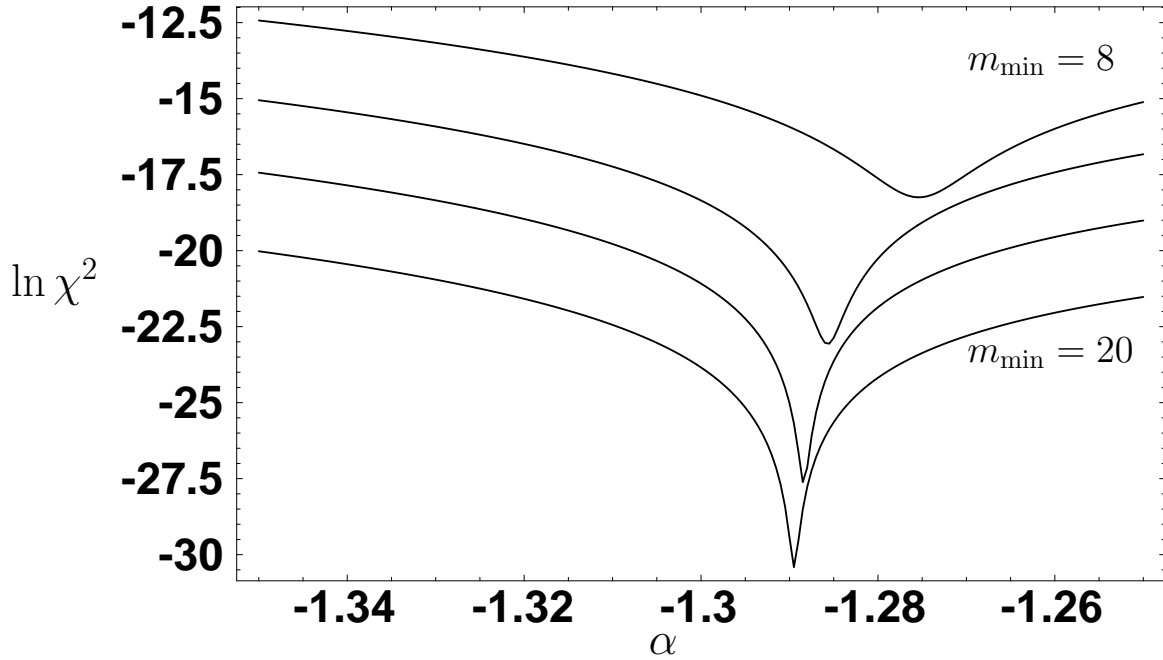


Figure 3: Effectiveness of the fit to the  $M_m$  in Eq. (15) using the function in Eq. (16). Note the dramatic spike at  $\alpha = -1.290$ .

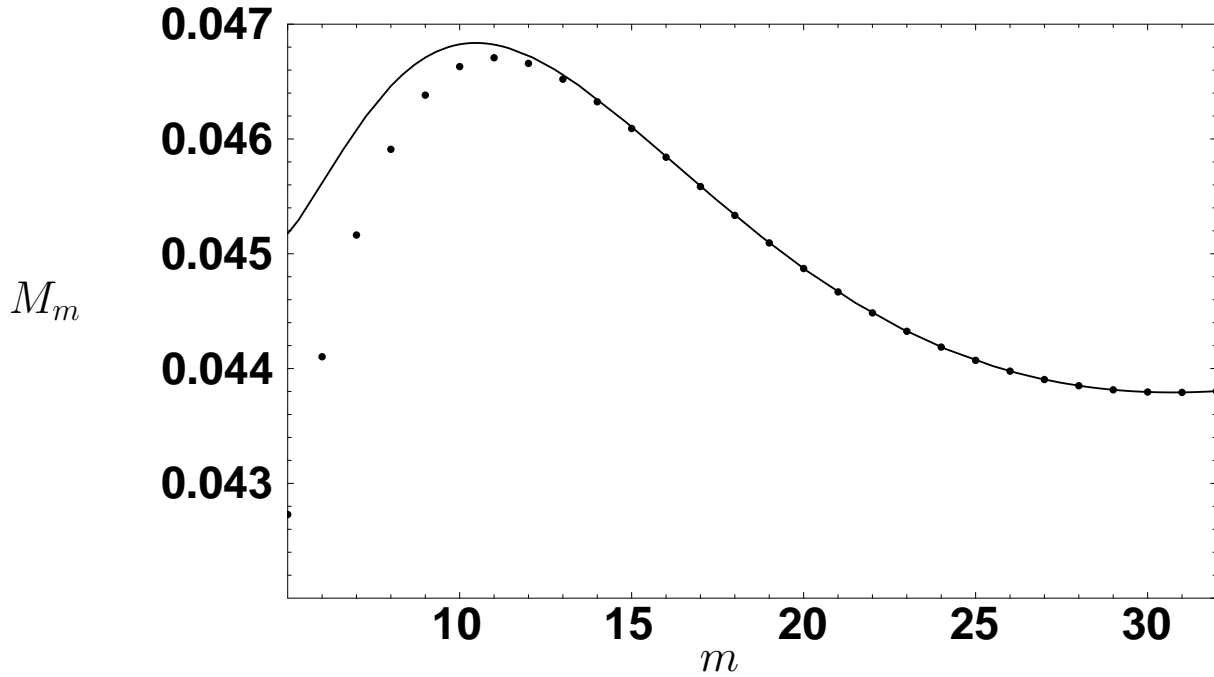


Figure 4: Optimal fit to the  $M_m$  in Eq. (15) (dots) using the function in Eq. (16) (curve), with  $\alpha = -1.290$ ,  $c_0 = 0.045514$  and  $c_1 = 0.000958 + 0.000185i$ . For most of the range of  $m$  the difference between the two is much smaller than the scale visible on this plot.

### 3.4 Borel summation

To conclude the analysis of the results, we apply the Shafer (generalised Padé) and Dingle (Borel summation) methods discussed briefly in Sec. 2.1 and compare the results with the exact eigenvalue  $\nu(\sigma)$  computed using the discretized eigenfunction method of Ref. [2] which is accurate to about six digits. Note that the full power of the Borel summation applied to the full computed series up to order  $\sigma^{64}$  is not (currently) testable, since this is the smallest term when it (and hence the expected errors) is of order  $(2e)^{-64/2} \approx 10^{-24}$ . Instead, we will consider quite large values of  $\sigma$ , where the smallest term is very close to the beginning of the series.

The only slight extension of the Dingle approach discussed in Sec. 2.1 concerns the modifying factor  $M_m$ . Since the asymptotic series now has three components, with  $p = 0, \pm 1$ , it is not clear whether each component should have a modifying factor. The point of view taken here is that a single modifying factor  $M_m$  is used for all three components. This choice is pragmatic; while it is probably more natural to modify each series separately, there is no method of extracting this information from the numerical data.

The results of the Borel summation are shown in Fig. 5. The bunch of lower solid curves are the Borel summed series, using five forward differences (see Sec. 2.1) and from two to four terms of the series before truncation. Note that the Borel summed function is consistent for relatively large  $\sigma$ , despite the obvious approximations made in approximating the series by so few terms. The dashed line is the result of a Shafer (quadratic Padé) approximation to the first 13 nonzero coefficients, as discussed in Sec. 2.1; the exact number of coefficients fitted makes little difference. These two interpretations of the power series are quite consistent. The dotted line is the true eigenvalue, computed as in Ref. [2]. It is extremely close to the Borel summed series for  $\sigma < 0.08$ , after which it is significantly higher.

The difference may be modelled by a function which is exponentially small for  $\sigma \rightarrow 0$ . The most obvious candidate (but one of many) is  $C \exp(-\sigma_0^2/\sigma^2)$ , which is roughly the magnitude of the smallest term, and is also the first expected “hyperasymptotic” correction. The remaining solid curve in Fig. 5 gives one of the Borel summed curves, plus this function with  $C = 0.09$ . The dot-dashed curve gives the equivalent result for the Shafer approximant. The result is a fit valid for roughly  $\sigma < 0.16$ , indicating that the exponential part of the correction has the right form.

It is reasonable to identify this exponentially small correction as the contribution of the generalised periodic orbit in Sec. 3.2. However, there is actually a fractal set of such generalised periodic orbits, starting from the critical point of the map and limiting to each orbit on the repeller. The orbit given in Sec. 3.2 is the most probable case, but other orbits have exponents which are arbitrarily close. The nontrivial task of summing these contributions is left to a future paper.

Incidentally, there exist rigorous results pertaining to Borel summation of asymptotic series [17]. The observation of hyperasymptotic corrections implies the presence of singularities in the complex noise domain, however it is difficult to understand what physical

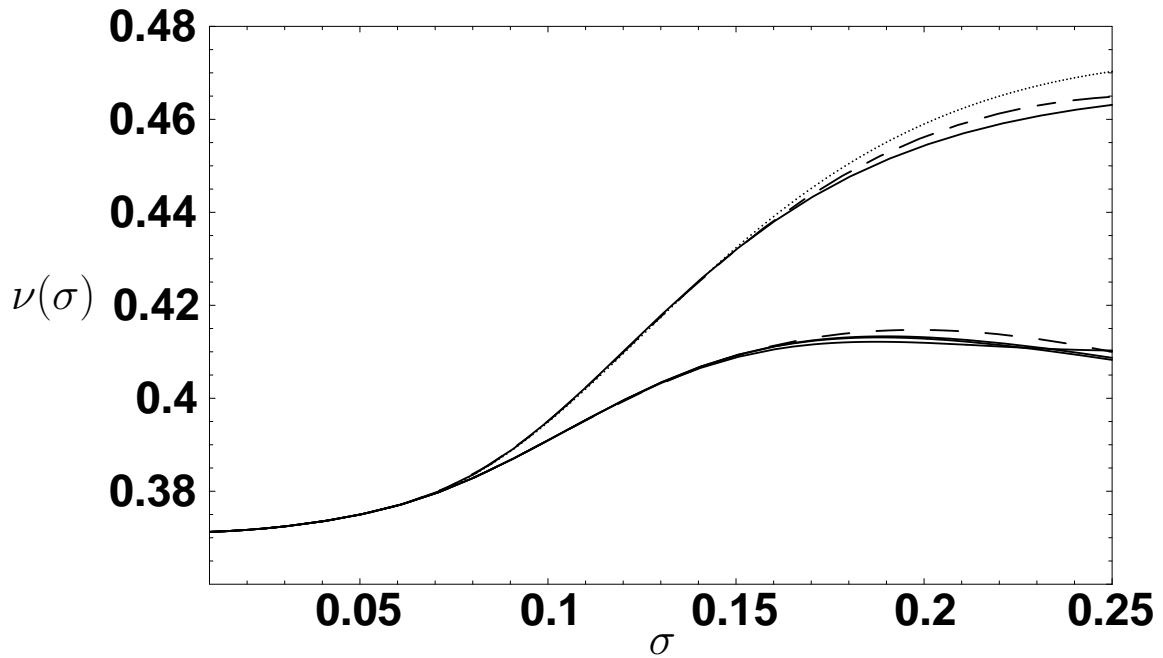


Figure 5: Borel summation of the series (lower solid curves) and Shafer approximant (dashed curve) together with an independent numerical calculation of the eigenvalue (dotted line). When an exponentially small function  $0.09 \exp(-\sigma_0^2/\sigma^2)$  is added to one of the former, the result is the upper solid line, and the dot/dash line respectively. These are much closer fits for larger values of the noise. Note that at the largest values of  $\sigma$  shown here, the asymptotic series is very rapidly divergent, with the minimum term given by  $1.44\sigma^2 \approx 0.09$ .

consequences this might have.

## 4 Conclusion

Periodic orbit theory of stochastic systems as presented in Ref. [4] has been used to compute the escape rate of a stochastically perturbed map to order 64 in the noise strength with sufficient precision to permit the theory of asymptotic expansions to be applied. Similar to a previous calculation of an exactly selfsimilar fractal, complex exponents appear, and the parameters in the expansion were found by a combination of analytic arguments and curve fitting. Although connections between this and the previous calculation were at a phenomenological level, the precise fit gives strong numerical evidence that the form of the expansion is correct to this order. Finally the Shafer approximation and Borel summation were performed on the series and compared with the known escape rate function, giving evidence for hyperasymptotic corrections of the same order as predicted by the theory of asymptotic expansions and independently by nonleading stationary points of the action.

In the future, the analytic connections proposed between the singulant and the probability of returning to the repeller from the critical point, and between the imaginary exponent and the spatial scaling factor of the repeller, should be verified by calculations on a variety of different systems. The remaining tentative connection, between the real exponent  $\alpha$  and the  $D_\infty$  dimension of the repeller would then either be verified or contradicted. The latter possibility is the most intriguing, since in that case  $\alpha$  could define a new “noise dimension”.

## Acknowledgments

The author is grateful for helpful discussions with Michael Berry, Predrag Cvitanović, Giovanni Gallavotti, Jon Keating, Jonathan Robbins and Niels Sørensgaard. This research was supported by the Nuffield Foundation, grant NAL/00353/G.

## References

- [1] P. Cvitanović, R. Artuso, R. Mainieri, G. Tanner and G. Vattay, *Classical and Quantum Chaos*, [www.nbi.dk/ChaosBook/](http://www.nbi.dk/ChaosBook/), Niels Bohr Institute (Copenhagen 2003).
- [2] P. Cvitanović, C. P. Dettmann, R. Mainieri and G. Vattay, *J. Stat. Phys.* **93**, 981 (1998).
- [3] P. Cvitanović, C. P. Dettmann, R. Mainieri and G. Vattay, *Nonlinearity* **12**, 939 (1999).

- [4] P. Cvitanović, N. Sørengaard, G. Palla, G. Vattay and C. P. Dettmann, Phys. Rev. E **60**, 3936 (1999).
- [5] G. Palla, G. Vattay, A. Voros, N. Sørengaard and C. P. Dettmann, Found. Phys. **31** 641 (2001).
- [6] C. P. Dettmann, Phys. Rev. E **59**, 5231 (1999).
- [7] J. P. Boyd, Acta Applic. Math. **56**, 1 (1999).
- [8] R. E. Shafer, SIAM J. Numer. Anal. **11**, 447 (1974).
- [9] M. V. Berry and C. J. Howls, Proc. Roy. Soc. London A, **430** 653 (1990).
- [10] R. B. Dingle *Asymptotic expansions: their derivation and interpretation* (Academic Press, London, 1973).
- [11] M. Abramowitz and I. A. Stegun *Handbook of mathematical functions* (National Bureau of Standards, 1964).
- [12] D. Bessis, J. S. Geronimo and P. Moussa, J. Stat. Phys. **34**, 75 (1984).
- [13] C. P. Dettmann and N. E. Frankel, J. Phys. A: Math. Gen. **26**, 1009 (1993).
- [14] C. P. Dettmann and N. E. Frankel, J. Stat. Phys. **72**, 241 (1993).
- [15] H. Saleur and D. Sornette, J. Phys. I **6**, 327 (1996).
- [16] P. Gaspard, J. Stat. Phys. **106**, 57 (2002).
- [17] G. H. Hardy *Divergent series* (Clarendon, Oxford, 1949).